Cancer Cell
Article

# Tumor Type-Dependent Function of the Par3 Polarity Protein in Skin Tumorigenesis

Sandra Iden,[1,3,5,*] Wilhelmina E. van Riel,[1] Ronny Schäfer,[1] Ji-Ying Song,[2] Tomonori Hirose,[4] Shigeo Ohno,[4] and John G. Collard[1,*]
[1]Division of Cell Biology I
[2]Division of Experimental Animal Pathology
The Netherlands Cancer Institute, 1066 CX Amsterdam, The Netherlands
[3]Cologne Cluster of Excellence in Cellular Stress Responses in Aging-Associated Diseases (CECAD), University of Cologne, 50931 Cologne, Germany
[4]Department of Molecular Biology, Yokohama City University Graduate School of Medical Science, Yokohama 236-0004, Japan
[5]Present address: Cologne Cluster of Excellence in Cellular Stress Responses in Aging-associated Diseases (CECAD), University Hospital of Cologne, Robert-Koch-Str. 21, 50931 Cologne, Germany
*Correspondence: sandra.iden@uk-koeln.de (S.I.), j.collard@nki.nl (J.G.C.)
http://dx.doi.org/10.1016/j.ccr.2012.08.004

## SUMMARY

**Cell polarization is crucial during development and tissue homeostasis and is regulated by conserved proteins of the Scribble, Crumbs, and Par complexes. In mouse skin tumorigenesis, Par3 deficiency results in reduced papilloma formation and growth. Par3 mediates its tumor-promoting activity through regulation of growth and survival, since *Par3* deletion increases apoptosis and reduces growth in vivo and in vitro. In contrast, Par3-deficient mice are predisposed to formation of keratoacanthomas, cutaneous tumors thought to originate from different cellular origin and frequently observed in humans. Par3 expression is reduced in both mouse and human keratoacanthomas, indicating tumor-suppressive properties of Par3. Our results identify a dual function of Par3 in skin cancer, with both pro-oncogenic and tumor-suppressive activity depending on the tumor type.**

## INTRODUCTION

Cell polarity is regulated by sets of polarity proteins including the Scribble, Par3, and Crumbs polarity complexes, which have been identified in invertebrates and show conserved functions in mammals (Assémat et al., 2008). The Par3 complex, consisting of partitioning-defective (Par)3, the Ser/Thr kinase atypical PKC (aPKC), and Par6, has the most ubiquitous function, being involved, for example, in apico-basal polarity, asymmetric cell division, and polarization of neuronal and T cells (Macara, 2004). Par3, aPKC, and Par6 can form a ternary complex, but in certain processes Par3 is excluded from the aPKC-Par6 domain through aPKC-mediated phosphorylation (Morais-de-Sá et al., 2010; Horikoshi et al., 2009). Par3 binds multiple proteins including the Rac-GEF Tiam1, thereby coupling Rac activation to Par polarity signaling. Cross-talk between polarity complexes and Rho GTPases is necessary to accomplish the cytoskeletal changes required for cell polarization (Iden and Collard, 2008).

Loss of polarity is considered a prerequisite for tumor formation and progression. In *D. melanogaster*, mutations in genes of the Scribble complex (*Scribble*, *Dlg*, and *Lgl*) cause loss of apico-basal polarity and neoplastic outgrowth when mutated or combined with *Ras* mutations (Bilder, 2004). In human tumors,

### Significance

Although loss of cell polarity is considered a prerequisite for tumor formation and progression, in vivo evidence demonstrating polarity protein function in mammalian tumorigenicity is limited. We show functional consequences of loss of the Par3 polarity protein in cancer. In skin, Par3 acts both as tumor promoter and tumor suppressor, depending on the tumor type involved. Par3 localizes aPKC and Ras signaling components to cell-cell contacts. Importantly, epidermal *Par3* deletion results in increased formation of Ras-induced keratoacanthoma. This tumor occurs frequently in humans, spontaneously or as an adverse effect of anticancer drugs. Chemical carcinogenesis in Par3-deficient mice provides a useful model for keratoacanthoma development relevant for human disease. Our data unravel a highly context-dependent contribution of Par3 to oncogenic processes.

the expression of polarity proteins is frequently altered though this seems to be highly context-dependent. Scribble complex proteins, similar to their tumor-suppressive function in invertebrates, show mainly reduced protein levels. In contrast, Par complex proteins are often upregulated in carcinoma (Nolan et al., 2008; Huang and Muthuswamy, 2010). Pro-oncogenic functions have been suggested particularly for aPKCι, because it seems required for transformation and tumorigenesis of pancreatic and lung cancer cells (Murray et al., 2011). In mice, Par3 deficiency is embryonically lethal (Hirose et al., 2006), and the function of Par3 during later development and in pathological situations is unknown.

Oncogenic factors such as UV radiation, chemicals, and pathogens as well as hereditary causes induce a variety of skin tumors including melanoma, basal cell carcinoma (BCC), squamous cell carcinoma (SCC), and keratoacanthoma (KA). To elucidate a potential function of the Par complex in oncogenic processes, we investigated the consequence of epidermal loss of Par3 on 7,12-dimethylbenz(a)anthracene (DMBA)-initiated and 12-O-tetradecanoylphorbol-13-acetate (TPA)-promoted skin tumorigenesis and identified tumor-promoting and -suppressing activities of Par3 in cutaneous tumors of clinical relevance.

## RESULTS

### Par3 Deficiency Inhibits Ras-Induced Tumorigenesis

To address a function of Par3 in the skin, we generated mice with conditional deletion of *Par3* in the epidermis and hair follicle (*K14-Cre*$^{+}$*;Par3*$^{flox/flox}$; hereafter *Par3* KO). These mice are viable and reached adulthood comparable to wild-type (WT) littermates. In control skin (*K14-Cre*$^{+}$*;Par3*$^{wt/wt}$, hereafter WT), Par3 is expressed throughout the interfollicular epidermis and the hair follicle and at much lower levels in the dermis. *Par3* KO tissue lacked epithelial Par3 immunoreactivity, and loss of Par3 was further confirmed in epidermal lysates of newborn and adult *Par3* KO mice (Figure 1A).

To examine if Par3 has a potential function in tumorigenesis, we applied a two-stage chemical skin carcinogenesis protocol. Topical treatment with the carcinogen DMBA induced oncogenic Ras mutations, and subsequent repeated treatments with the phorbol ester TPA promoted outgrowth of initiated cells resulting in benign papillomas in WT mice about 7 weeks after initiation. Interestingly, papilloma formation was delayed by about 3 weeks in *Par3* KO mice (Figure 1B), and tumor multiplicity was strongly reduced (Figures 1C and 1E; Table S1 available online). Moreover, tumors that did form grew slower in the absence of Par3 (Figure 1D), indicating that Par3 promotes Ras-induced tumor formation and growth. Typical papillomas in WT mice showed exophytic growth of squamous cells (Figure 1F). To prepare tissue lysates, we dissected from same mice both normal skin and tumors and repeated this for multiple WT and *Par3* KO littermates. The analysis of Par3 and aPKC expression in nontumor and tumor tissue lysates revealed robust levels of Par3 and aPKC in WT tumors, whereas Par3 protein was undetectable in *Par3* KO skin and tumors (Figure 1G). Together, these functional and biochemical data suggest a tumor-promoting function of Par3 in Ras-induced papillomas.

To address the mechanism of reduced tumor formation and growth in *Par3* KO mice, we tested the involvement of Par3 in epidermal proliferation and apoptosis in response to DMBA/TPA treatment of the skin. After single DMBA and subsequent dual TPA treatment, as measured by BrdU incorporation, proliferation was significantly reduced in *Par3* KO compared to WT epidermis (Figure 2A). Furthermore, Par3-deficient epidermis showed a significant increase in cells positive for cleaved caspase-3, which identifies apoptosis (Figure 2A), normally a rare event in skin. We isolated skin keratinocytes from mice with loxP-flanked Exon3 of *Par3* (Hirose et al., 2006) to further address a function of Par3 in cell survival and proliferation. In keratinocytes, the 180 kDa splice variant of Par3 shows highest expression, and self-excising Cre recombinase efficiently deleted *Par3* (Figure 2B). We expressed oncogenic Ras (RasV12) in cells (Figure 2C) and studied the role of Par3 in Ras-induced resistance to contact-mediated growth inhibition. Upon calcium switch (elevation from 20 μM $Ca^{2+}$, termed low calcium [LC], to 2 mM $Ca^{2+}$, termed normal calcium [NC]), which induces cadherin-mediated intercellular adhesion, RasV12 enabled keratinocytes continue to grow despite prolonged incubation at NC. In contrast, Par3-deficient cells showed attenuated growth (Figures 2D and 2E), suggesting that Par3 is required for Ras signaling to overcome differentiation-induced cell cycle arrest. This was not due to differential expression of major adherens junction (AJ) components because loss of Par3 did not affect the moderate Ras-mediated downregulation of E-cadherin and other AJ-associated proteins tested (Figure S2H). In addition, Par3-deficiency reduced the ability of RasV12 cells to form colonies in matrigel (Figure 2E) or soft-agar (data not shown), further supporting a growth-promoting function of Par3.

We further investigated whether Par3 is involved in activation of the phosphatidylinositol-3 kinase (PI3K)/Akt and MEK/ERK pathways, main modules mediating cell survival, proliferation, and apoptotic resistance in Ras-mediated skin tumorigenesis (Kern et al., 2011). Par3-deficient keratinocytes indeed exhibit consistently reduced ERK activation upon Ras expression and/or TPA treatment (Figures 2F and 2G) and reduced Akt activation upon Ras expression compared to WT cells (Figure S2B). Moreover, as in carcinogen-exposed skin, apoptosis was increased in starved, EGF-, or TPA-treated *Par3* KO keratinocytes as evidenced by caspase-3 and Parp1-cleavage (Figure 2H). Other stimuli such as heat shock and growth factor deprivation similarly induced a stronger apoptotic response in *Par3* KO than in WT cells (Figure S2D; data not shown). Increased Bax conformational change and caspase-9 processing in *Par3* KO cells indicated activation of the intrinsic, mitochondria-dependent apoptotic pathway in the observed apoptotic phenotype (Figures 2I, S2E, and S2F). Finally, cyclin D1 levels in *Par3* KO cells were lower than in WT cells (Figure S2C). This difference was further increased upon expression of oncogenic Ras, known to induce cyclin D1 expression (Filmus et al., 1994). Together, these results indicate that Par3 is required for Ras-induced tumor growth and promotes ERK- and Akt-mediated growth and survival signals that counterbalance apoptotic signaling.

### Par3 Interacts with and Localizes aPKC in Cultured Keratinocytes

Because Par3 has been shown to act together with aPKC in several cellular systems, we analyzed the subcellular localization of Par3 and aPKC in keratinocytes. At NC, Par3 was

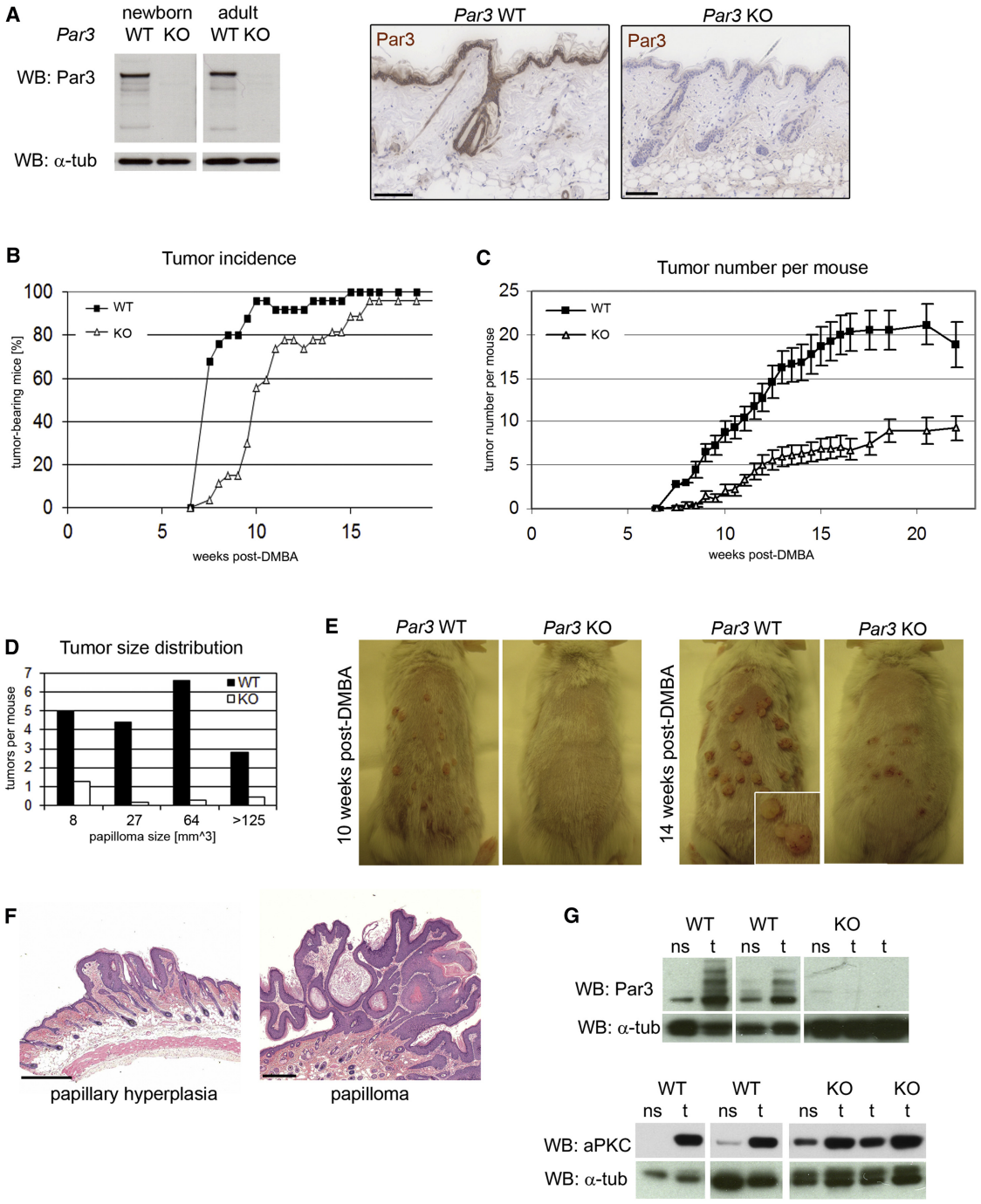


**Figure 1. Mice with Epidermal *Par3* Deletion Show Reduced Ras-Mediated Tumorigenesis**

(A) Western blot against Par3 and α-tubulin from epidermal lysates (left: epidermis from newborns; right: epidermis from 8 weeks old mice) and immunohistochemical Par3 staining of adult *K14-Cre*$^{+}$;*Par3*$^{wt/wt}$ (WT) or *K14-Cre*$^{+}$;*Par3*$^{flox/flox}$ (*Par3* KO) mice (right). Scale bars, 100 μm.

(B) Tumor incidence, indicated by percentage of tumor-bearing mice, in WT and epidermal *Par3* KO mice. n(WT) = 25, n(KO) = 27.

(C) Average number of tumors per mouse in WT and epidermal *Par3* KO mice (mean ± SEM).

(D) Tumor volume (length × width × height) in WT mice and epidermal *Par3* KO mice. Representative data are shown for 14.5 weeks post-DMBA.

(E) Representative photographs of TPA-treated WT and epidermal *Par3* KO mice 10 and 14 weeks after tumor initiation.

(F) Histologic sections of papillary hyperplasia and papilloma in WT mice, H&E. Scale bars, 500 μm.

(G) Western blot analysis of Par3 and aPKC expression in lysates of WT and *Par3* KO skin and tumors. Vertical white lines indicate that lanes were removed between the samples shown. ns, normal skin; t, tumor tissue; α-tub, α-tubulin.

See also Figure S1.

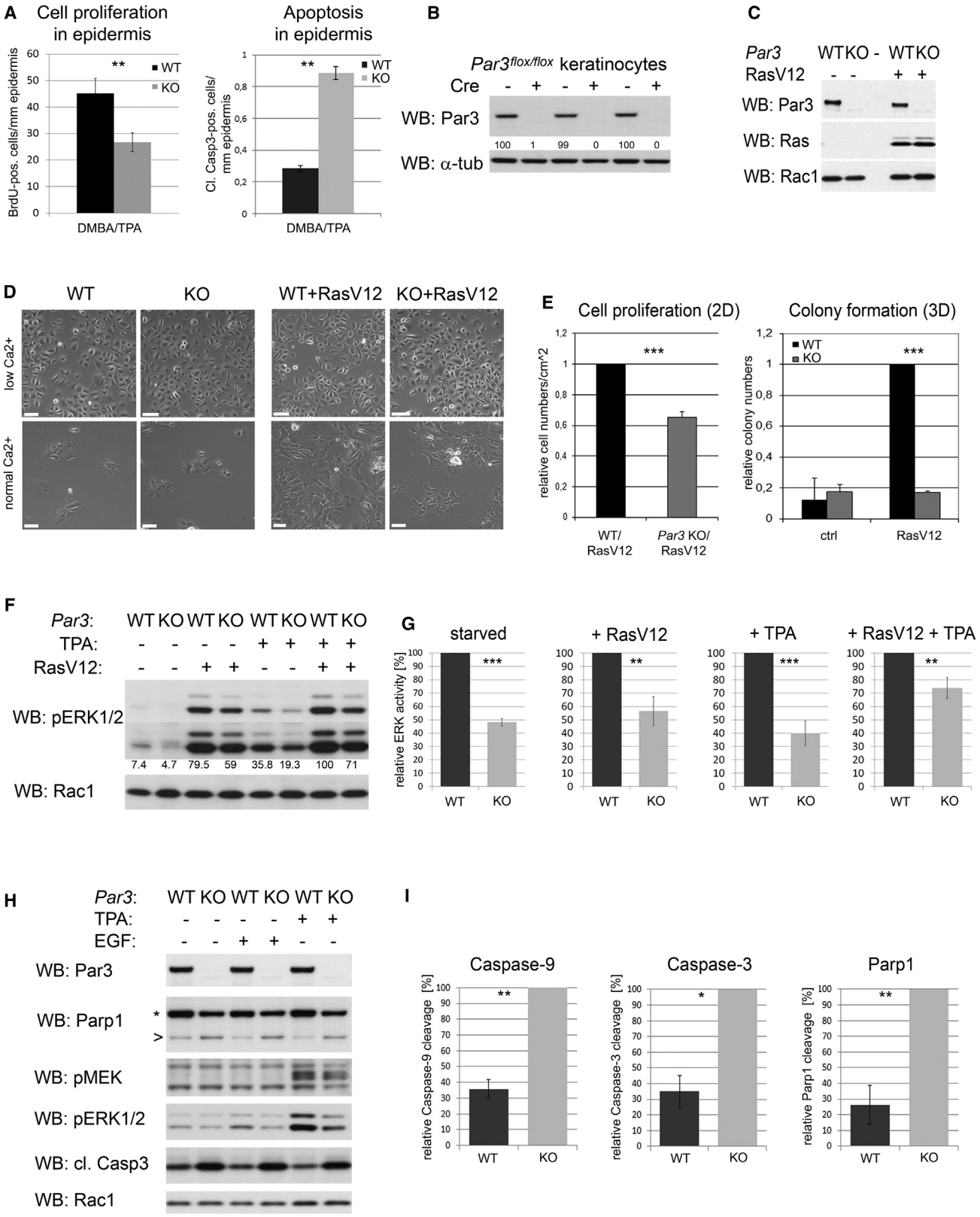


**Figure 2. Reduced Proliferation and Cell Survival and Increased Apoptosis upon Epidermal *Par3* Deletion**

(A) Back-skin of mice was treated once with DMBA and twice with TPA with a 3 day interval. Proliferation and apoptosis 24 hr after last treatment was quantified based on immunohistochemical analyses (mean ± SEM) (see Experimental Procedures for details).

predominantly found at ZO-1-positive cell-cell contacts of WT cells, whereas in *Par3* KO cells it was not (Figure 3A). The ZO-1 pattern was discontinuous in *Par3* KO cells in early phases of junction formation indicating impaired tight junction maturation upon loss of Par3 (6 hr NC; Figure 3A), which could be restored by myc-PAR3 expression (Figure S2A). In contrast, 48 hr after calcium switch ZO-1 distribution was comparable to WT cells (data not shown), indicating a temporary requirement of Par3 in initial steps of tight junction (TJ) formation as described for other epithelial cell types (Chen and Macara, 2005). Immunostaining revealed colocalization of Par3 and aPKC at keratinocyte TJs (Figure 3B), and co-immunoprecipitation revealed binding of both endogenous proteins in WT keratinocytes (Figure 3C), indicating the presence of a functional Par3-aPKC complex. In WT cells, we found aPKC localization at newly formed cell-cell contacts (30 min and 2 hr at NC) and at established intercellular junction of multilayered keratinocytes (3 days at NC on permeable supports) (Figure 3D). In *Par3* KO cells however, aPKC showed a diffuse cytoplasmic distribution and was absent at cell-cell contact sites, both shortly after calcium switch and in multilayers with established TJs (Figure 3D). As total aPKC levels are unaffected by *Par3* deletion (Figure 3C), our data suggest that Par3 is required for proper aPKC localization to intercellular contacts in cultured keratinocytes. Interestingly, similar to myc-PAR3, expression of membrane-targeted aPKC (aPKC-CAAX) could restore active ERK levels in *Par3* KO keratinocytes after starvation or when expressing RasV12 combined with TPA stimulation (Figures 3E and 3F). Furthermore, similar to *Par3* deletion, siRNA-mediated depletion of aPKC impaired TPA-induced ERK activation (Figure S3A) and resulted in increased apoptosis (Figure S3B), indicating that aPKC likely contributes to Par3-dependent ERK stimulation and survival.

## Altered Localization of Ras-MAPK Pathway Components upon Loss of Par3

To assess how Par3 dysfunction impacts survival and growth signaling, we analyzed the subcellular localization of crucial components of the Ras signaling pathway in control and Par3-deficient epidermis, papillomas, and keratinocytes. Interestingly, endogenous Ras and its GEF Sos2 localized to cell-cell contacts of control epidermis and papilloma tissue in a pattern similar to that of Par3 (Figure 4A, top). This specific localization, however, was strongly diminished in *Par3* KO tissue (Figure 4A, bottom), suggesting that Par3 mediates the localization of Ras pathway components to intercellular adhesions. In primary keratinocytes, endogenous Ras and Par3 indeed colocalized at cell-cell contacts (Figure 4B) and both exogenous oncogenic RasV12 and endogenous Sos2 colocalized with ZO-1 (Figures 4B and 4C), indicating that they associate with TJs. RasV12 further codistributed with Par3 at cell-cell contacts in WT keratinocytes (Figure 5A, top), whereas this localization was diminished in *Par3* KO keratinocytes (Figure 5A, middle). Importantly, RasV12 localization to intercellular contacts could be restored by expression of exogenous human myc-PAR3 in *Par3* KO cells (Figure 5A, bottom), suggesting that Par3 mediates localization of active Ras to these sites. In line with the in vivo data (Figure 4A) also Sos2 displayed Par3-dependent cell-cell contact localization as evident by loss of Sos2 from these sites in *Par3* KO keratinocytes cultured at NC (Figure 5B). Finally, next to cytoplasmic and nuclear pools we observed the active form of the downstream effector ERK1/2 (pERK1/2) at cell-cell contacts in WT cells (Figure 5C), colocalizing with aPKC (Figure 5D). Similar to Ras and Sos2, pERK1/2 was not found at intercellular contacts of *Par3* KO cells (Figures 5C and 5D, right). Ras, Sos2, MEK, and ERK protein levels were unaffected by loss of Par3 in keratinocytes (Figure 5E), excluding that Par3 regulates the expression of these proteins. Together, the above data suggest that junctional Par3 mediates localization of Ras pathway components and thereby helps to assemble a functional, signaling-competent platform at intercellular contacts that efficiently stimulates growth and survival signaling in papillomagenesis.

## Increased Formation of Keratoacanthoma in Par3-Deficient Mice

To examine if Par3 is important for the progression of papillomas to SCCs, mice were inspected thoroughly during the experiment. While papillomas, the predominant tumors of WT mice, showed clear exophytic growth with a narrow stem connecting tumor mass and skin (Figures 1F and S1A), *Par3* KO mice often developed tumors with initially glossy surface that rapidly grew inward (Figures 6A and 6B). This caused experiment termination 22 weeks postinitiation as tumor sizes reached >1 cm. At dissection we noticed deep protrusion of tumors into the dermis and presence of strong vascularization at the base. These tumors were histologically identified as keratoacanthoma (KA), a tumor rarely observed in mice but common in human, with typical crater-like morphology, broad tumor base and a keratin-filled center (Figures 6B, S1D, S1H, and S1I). Histopathological

(B) Western blot of cultured keratinocytes upon Cre-mediated *Par3* deletion. The 180kDa band shown reflects the dominantly expressed splice variant in keratinocytes (WT: $Par3^{fl/fl}$, KO: $Par3^{fl/fl}$ + self-excising Cre). Numbers indicate the relative Par3 expression after normalization to loading control α-tubulin.
(C) Western blot of transduced oncogenic Ras (RasV12) in WT and *Par3* KO keratinocytes. Rac served as loading control.
(D) Phase-contrast micrographs of WT and *Par3* KO keratinocytes either untreated (left) or upon expression of RasV12 (right) at growth (low $Ca^{2+}$, top) and differentiating (normal $Ca^{2+}$, bottom) conditions. Scale bars, 20 μm.
(E) Proliferation and colony formation induced by oncogenic Ras. Cell proliferation on culture plates (left) and colony formation in 3D upon seeding single cell suspensions of RasV12-infected WT and *Par3* KO keratinocytes into matrigel and incubation for 10 days at NC (right) was assessed (mean ± SD).
(F) Western blot analysis of total cell lysates to detect ERK activation in WT and *Par3* KO cells (bottom: longer exposure of top pERK blot). Serum-starved keratinocytes were infected with oncogenic Ras and/or treated with 0.68 μM TPA for indicated time points.
(G) Quantification of F, ERK activation upon loss of Par3 in starved, Ras-expressing and TPA-treated cells ($n \geq 4$) (mean ± SEM).
(H) WT and *Par3* KO cells were cultured at NC for 36 hr, serum-starved and treated with TPA or EGF. Apoptosis was indicated by caspase-3 and Parp1 cleavage, ERK pathway activity by pMEK and pERK levels. Asterisk: full-length Parp1; arrow: cleaved Parp1 fragment.
(I) Quantification of apoptosis markers upon starvation ($n \geq 3$) (mean ± SEM). Representative western blots for caspase-9 are provided in Figure S2E. *$p < 0.05$; **$p < 0.01$.
See also Figure S2.

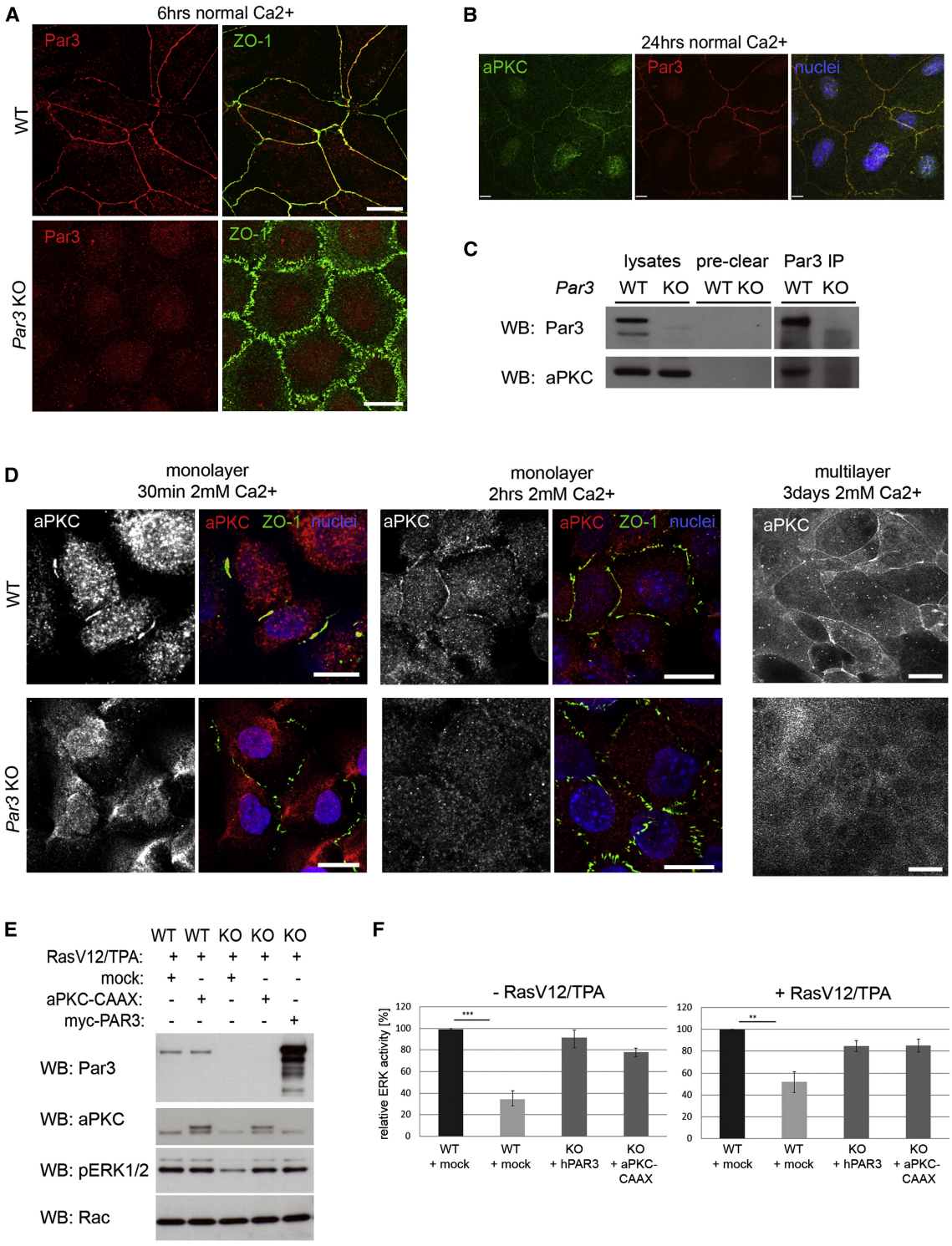


**Figure 3. Par3 Interacts with aPKC and Mediates Cell-Cell Contact Localization of aPKC in Keratinocytes**

(A) Endogenous Par3 and ZO-1 immunostaining 6 hr after calcium switch to NC. Continuous, thin lines of ZO-1 immunoreactivity indicate matured tight junctions. Scale bar, 10 μm.

(B) Co-immunostaining of aPKC and Par3 in WT keratinocytes cultured for 24 hr at NC. Scale bar, 10 μm.

(C) Co-immunoprecipitation of endogenous Par3 and aPKC in WT keratinocytes 6 hr after $Ca^{2+}$ switch (see Supplemental Experimental Procedures for details). Vertical white lines indicate that lanes were removed between the samples shown.

(D) Immunostaining against aPKC and ZO-1 in WT and *Par3* KO keratinocytes. Various time points after calcium switch were analyzed as indicated on top. Scale bars, 10 μm.

analyses confirmed that at termination *Par3* KO mice had formed 6.63 KAs per mouse (91% of mice KA-positive; Table S1), whereas in WT mice only 0.53 KAs per mouse were detected (27% of WT mice KA-positive; Table S1), which were too small to be macroscopically classified as such. Formation of SCCs was in total rare at week 22 but *Par3* KO mice appeared not to be prone to SCC formation. WT mice had slightly increased SCC formation (0.4 SCCs per mouse, 20% of WT mice SCC-positive; Table S1) compared to *Par3* KO mice (0.18 SCCs per mouse, 18% of KO mice SCC-positive; Table S1). Of note, all tumors tested were positive for *Ras* codon 61 mutations (Figure S4A) described to be induced by DMBA (Finch et al., 1996), indicating that KAs were also induced by oncogenic Ras signaling. Lack of Par3 expression was confirmed in all tested *Par3* KO-derived tumors (data not shown), excluding the possibility that KAs developed from rare cells that had escaped Cre-mediated *Par3* deletion. The remarkably increased incidence and accelerated appearance of KAs in *Par3* KO mice (Figures 6C and 6D; Table S1) contrasted the reduced papilloma formation in these mice (Figures 1B, 1C, and 6D; Table S1), indicating a dual function of Par3 in development of skin tumors dependent on the tumor type.

To address further the molecular functions of Par3 in the skin and the different skin tumors, we explored the subcellular localization of Par3 and aPKC in skin tissue. Par3 was robustly expressed in epidermis and papilloma tissue, where it localized to sites of cell-cell contacts (Figure 6E, top), but was lost in the few KAs of WT mice (Figure 6E, top). Similar to cultured keratinocytes (Figure 3D), we found a requirement of Par3 for junctional localization of aPKC in vivo, as aPKC was strikingly mislocalized to the cytoplasm in Par3-deficient epidermis and tumors as well as in the rare WT KAs that displayed reduced Par3 levels (Figure 6E, middle and bottom). Instead, ZO-1 showed normal TJ distribution in WT and *Par3* KO epidermis and appeared cortically distributed but scattered both in WT papilloma and *Par3* KO KAs (Figure S4D), suggesting Par3-independent ZO-1 localization in this context. Since KAs also develop in humans, we further investigated possible similarities between Ras-induced mouse tumors and patient-derived KAs. Quantitative analyses of sections of non-diseased human skin and 10 KA tumors revealed that PAR3 was clearly detectable in basal and suprabasal layers of healthy epidermis and in epidermis adjacent to tumors, partially colocalizing with E-CADHERIN, ZO-1 and aPKC (Figure S4C). However, its expression was significantly reduced in the tumor epithelium of KAs (Figures 6G, 6H, and S4B), similarly as found in murine WT KAs. In contrast, analysis of human SCCs did not reveal significantly reduced PAR3 expression (Figure 6H, bottom panel; Figure S4B, right panel), in line with the lack of significant alterations of SCC incidence in *Par3* KO mice (Table S1). From these data we conclude that Par3 expression and localization differs in papillomas and KAs, consistent with the differential tumor outcome in mice with *Par3* deletion (Figures 1 and 6; Table S1). Analysis of keratinocytes cultured at LC versus NC indicated that depending on the cellular context and presence of cell-cell contacts Par3 is differentially required for MAPK signaling (Figure S3D). We therefore assessed if a differential activity of crucial MAPK components could be confirmed in tumor tissues. Interestingly, we observed abnormally high levels of phosphorylated active CRaf in a distinct vesicular pattern in basal layers of *Par3* KO epidermis as well as Par3-deficient KAs (Figure 7A, bottom). In contrast, in WT epidermis this active CRaf was moderately detected at cell-cell contacts of the suprabasal layers, in few vesicular structures in the basal layer and was only very weakly present in WT papilloma tissue (Figure 7A, top). These data implicate Par3 in CRaf activation and/or localization in the context of KA formation. The abundance of active CRaf in intracellular vesicles has been reported previously (Rizzo et al., 2001) and could be recapitulated in vitro in *Par3* KO but not WT keratinocytes cultured at LC (Figure 7B), suggesting that in the absence of profound intercellular adhesions cytoplasmic Par3 serves to restrict CRAF activity.

Together, the above data indicate that the tumor-suppressive function of Par3 in KA formation involves regulation of CRaf and illustrate that polarity proteins contribute to clinically relevant pathologies.

## DISCUSSION

Our functional tumorigenicity studies reveal a hitherto unknown role of the Par3 polarity protein in mammalian cancer, i.e., a tumor-promoting function in papilloma formation and tumor-suppressive activity in KA formation. Previously, polarity proteins of the Scribble complex have been implicated in tumor suppression in D.*melanogaster,* in D.*rerio* and recently in mice (Bilder, 2004; Reischauer et al., 2009; Zhan et al., 2008; Pearson et al., 2011). Similarly, Par4/LKB1 shows tumor-suppressive activity (Vaahtomeri and Mäkelä, 2011), and loss of Par4/LKB1 associated with impaired epithelial integrity synergizes with oncogenic c-*myc* induced mammary tumorigenesis (Partanen et al., 2012). In the DMBA/TPA tumor model involving Ras mutations, we found that Par3 can serve either as a tumor promoter in papilloma formation or a tumor suppressor in KA formation. Par3-deficient mice did not develop spontaneous skin tumors, indicating that Par3 dysfunction in mice alone is not sufficient to drive tumorigenesis. Malignant transformation of papillomas by local invasion into the stroma was observed in 45% of the relatively small tumors found in *Par3* KO mice and in 33% of the abundant larger tumors of WT mice (Table S1), suggesting that loss of Par3 promotes Ras-mediated metastasis of tumor cells as found in *Drosophila* (Pagliarini and Xu, 2003). Similarly, local invasion by KAs was exclusively observed in *Par3* KO mice (36%; Table S1) although we cannot exclude that this is the result of the earlier onset of KAs in these mice.

Isolated epidermal keratinocytes appear to recapitulate well what is occurring during papillomagenesis. In the absence of Par3, both carcinogen-exposed epidermis and cultured

(E) Expression of myc-hPAR3 and of membrane-targeted aPKC (aPKC-CAAX) in *Par3* KO keratinocytes to restore ERK activity. RasV12-expressing cells were cultured at NC and treated with TPA.
(F) Quantification of ERK activity in WT and KO *Par3* KO keratinocytes transfected with control plasmid, myc-hPAR3 or aPKC-CAAX, either untreated (left) or upon expression of RasV12 and subsequent TPA treatment (right) (n = 3). Mean ± SEM; $^{**}p < 0.01$; $^{***}p < 0.001$.
See also Figure S3.

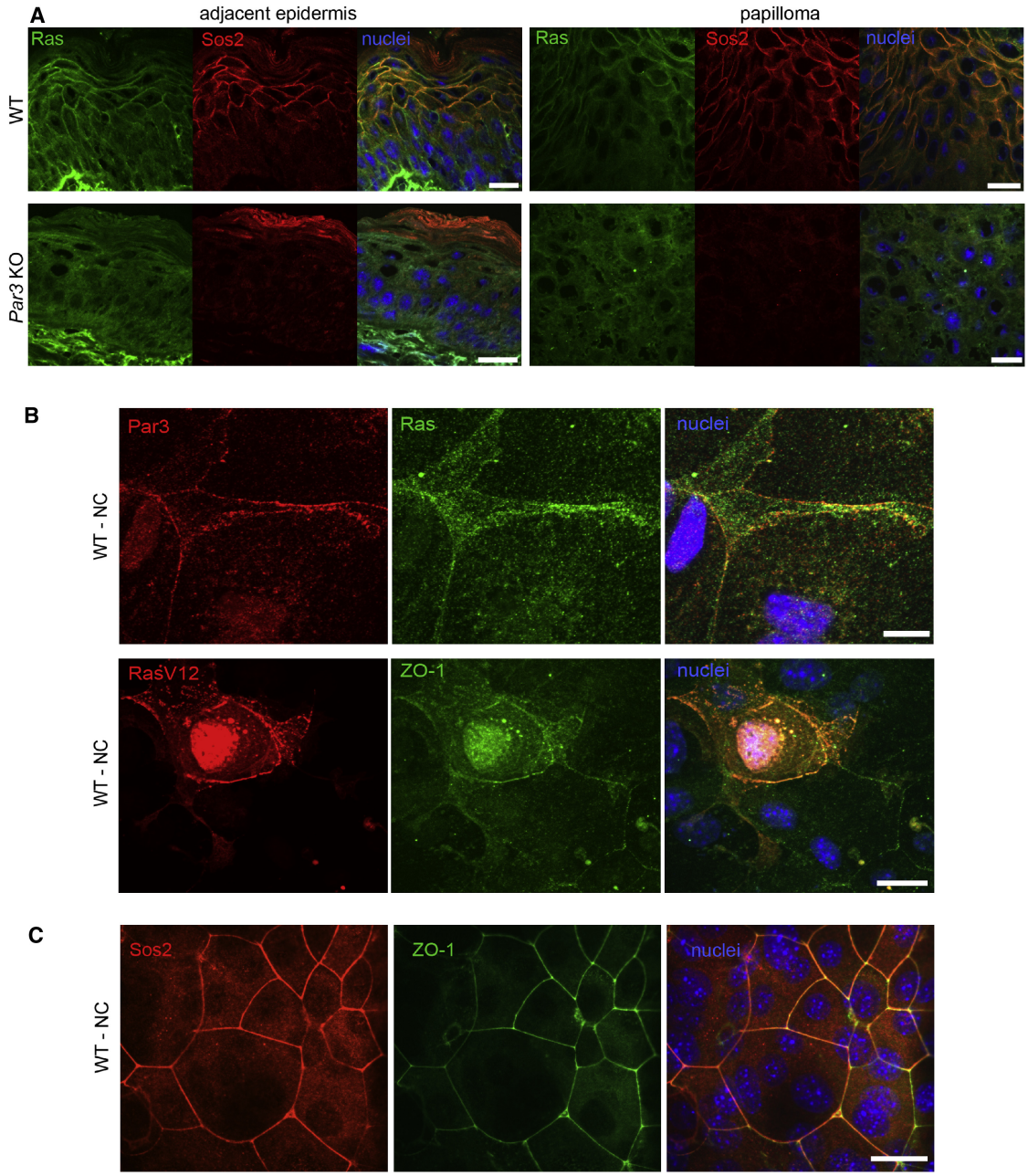


**Figure 4. The Localization of Ras and the RasGEF Sos2 to Cell-Cell Contacts Is Par3-Dependent**

(A) Immunostaining of Ras and the Ras-GEF Sos2 in murine epidermis adjacent (left) to papillomas (right) in WT (top) and *Par3* KO (bottom) tissues. Scale bars, 20 μm.

(B) Co-immunostaining of endogenous Par3 and Ras, and of oncogenic Ras (HA-RasV12, stained with HA-tag antibodies) with the endogenous, TJ-associated protein ZO-1 in WT keratinocytes. Scale bars, 20 μm.

(C) Co-immunostaining of the endogenous Ras-GEF Sos2 with ZO-1 in WT keratinocytes 48 hr after switch to NC. Scale bars, 20 μm.

keratinocytes show reduced proliferative responses and higher apoptotic sensitivity (Figure 2). Par3 likely promotes Ras-induced ERK- and Akt-mediated cell growth and apoptotic resistance giving rise to papillomas. To date, no direct molecular link between Par3 and Ras signaling has been reported. Recently, direct binding of Par3 to PI3K, PTEN and phosphoinositides and a positive feedback of the Par3 complex to PI3K has been postulated in the context of axon formation and establishment of plasma membrane polarity (Itoh et al., 2010; Yoshimura et al., 2006; Cain and Ridley, 2009). Our findings of reduced Akt activity upon loss of Par3 in keratinocytes suggest that such interactions also sustain survival signals in skin tumorigenesis. We further provide evidence that loss of Par3, concomitant with reduced survival signaling, results in activation of the

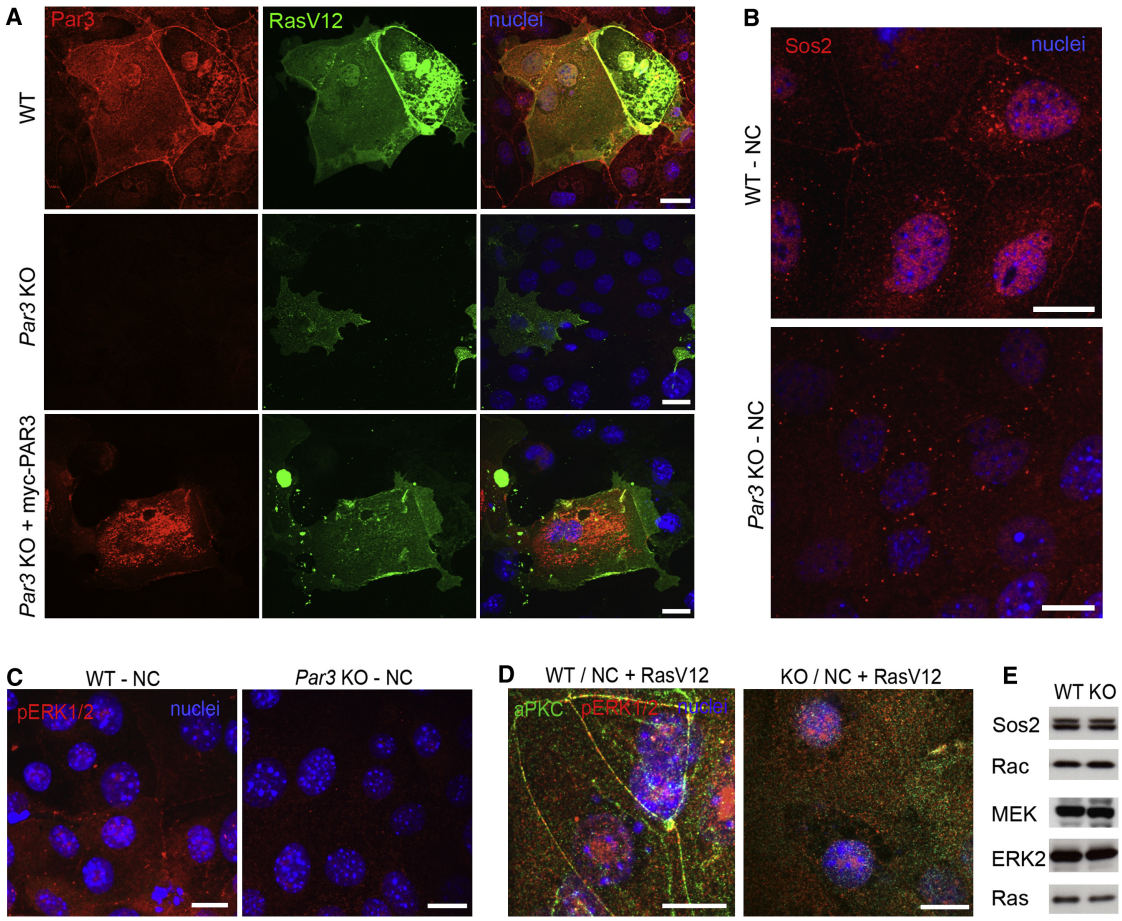


**Figure 5. Mislocalization of Ras Pathway Components upon Loss of Par3 in Epidermis, Skin Tumors, and Keratinocytes**

(A) Immunofluorescent co-staining of RasV12, stained with HA-tag antibodies, and Par3 in WT keratinocytes (top), in *Par3* KO cells (middle), and in *Par3* KO keratinocytes expressing myc-PAR3 (bottom). All cells were cultured at NC. Scale bars, 20 μm.

(B) Immunofluorescent staining of Sos2 to depict its localization in WT and *Par3* KO keratinocytes. Scale bars, 20 μm.

(C) Immunofluorescent staining of phosphorylated ERK1/2 in WT (left) and *Par3* KO (right) keratinocytes to detect sites of high ERK activity. Scale bars, 20 μm.

(D) Immunofluorescent staining of aPKC and active ERK (pERK1/2) to depict colocalization in WT and *Par3* KO keratinocytes expressing RasV12 and cultured at NC. Scale bars, 20 μm.

(E) Western blot analysis of Sos2, MEK, ERK2, and Ras and Rac protein levels in WT and *Par3* KO keratinocytes.

intrinsic mitochondria-dependent apoptotic pathway (Figures 2I, S2E, and S2F), which has earlier been implicated in balancing skin tumor growth in the DMBA/TPA tumor model (Cho et al., 2001) and mediating UV-induced cell death in human keratinocytes (Van Laethem et al., 2004).

We and others have shown that Par3 can cross-talk to Rho GTPase signaling through interaction with the Rac-GEF Tiam1. Tiam1 and Rac collaborate with the Par3-aPKC complex to regulate TJ biogenesis and persistent migration of keratinocytes (Iden and Collard, 2008). Similar to Tiam1-depleted cells, *Par3* KO keratinocytes are impaired in scratch-induced wound closure (Figure S2G). Interestingly, deletion of Tiam1 or Rac1 also suppresses Ras-induced papilloma formation (Malliri et al., 2002; Wang et al., 2010), suggesting that Par3 and Tiam1/Rac1 function is coupled not only during cell polarization but also in tumorigenic events downstream of Ras. Considering the striking resemblance between papilloma phenotypes upon deletion of Tiam1, Rac1 or Par3, and our previous findings that Tiam1/Rac regulates the Par3 complex in polarizing keratinocytes (Pegtel et al., 2007) we speculate that Par3 acts at the level of Tiam1/Rac in papillomagenesis. Of note, the increased KA incidence in *Par3* KO mice has not been observed in Tiam1- and Rac1-deficient mice, indicating that the tumor-suppressive effect of Par3 on KA formation is not coupled to Tiam1/Rac signaling. Moreover, in contrast to increased SCC formation in Tiam1-KO mice (Malliri et al., 2002), we could not detect a significant contribution of Par3 expression on SCC formation (Table S1). A recent report implicates the RAS/RAF/MAPK axis in formation of human SCC (Reuter et al., 2009). Due to the rapidly growing KAs, which appear much earlier than SCCs, animals needed to be sacrificed before profound SCC onset, preventing a statistically validated conclusion on the function of Par3 in SCC formation. Hence, considering the different kinetics of SCC and KA formation, we cannot exclude that SCC initiation is altered upon loss of Par3. However, we did not detect significant differences in the expression of PAR3 in

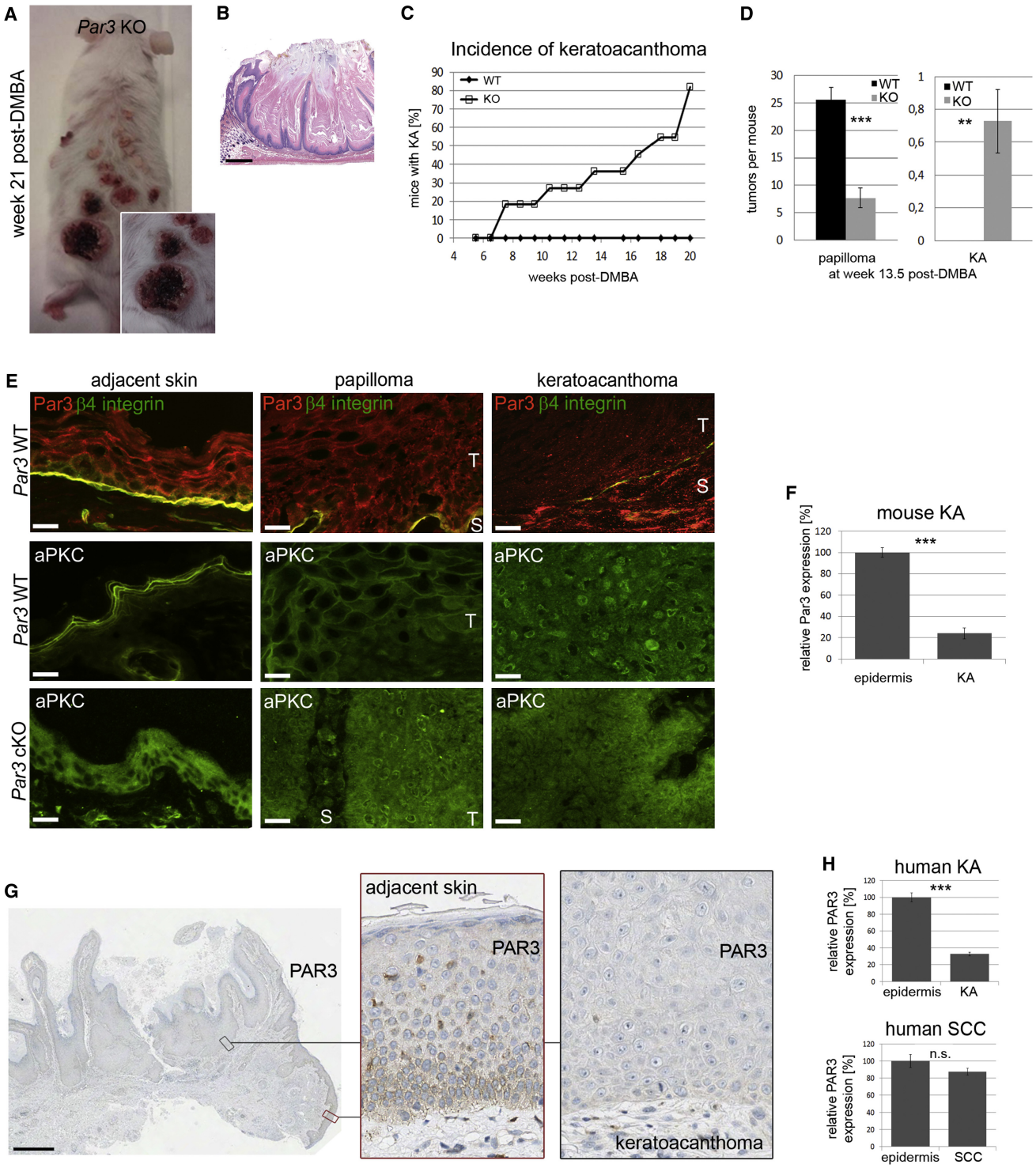


**Figure 6. *Par3* cKO Mice Develop Keratoacanthomas**

(A) Representative photograph of keratoacanthomas in *Par3* KO mice 21 weeks post-DMBA.

(B) Representative H&E staining of KA cross-section. Scale bar, 1 mm.

(C) KA incidence based on macroscopic analysis of WT and *Par3* KO mice. For histologic analyses, see Table S1.

(D) Number of papillomas versus KAs per mouse based on macroscopic analysis at week 13.5 post-DMBA. For histologic analyses, see Table S1.

(E) Par3 and aPKC immunostaining in cryosections of mouse epidermis, papilloma and KA. β4 integrin signal reflects the epidermal-dermal border. Scale bars, 20 μm. T, tumor; S, stroma.

(F) Quantification of Par3 protein expression in KAs of WT mice and epidermis adjacent to the tumors.

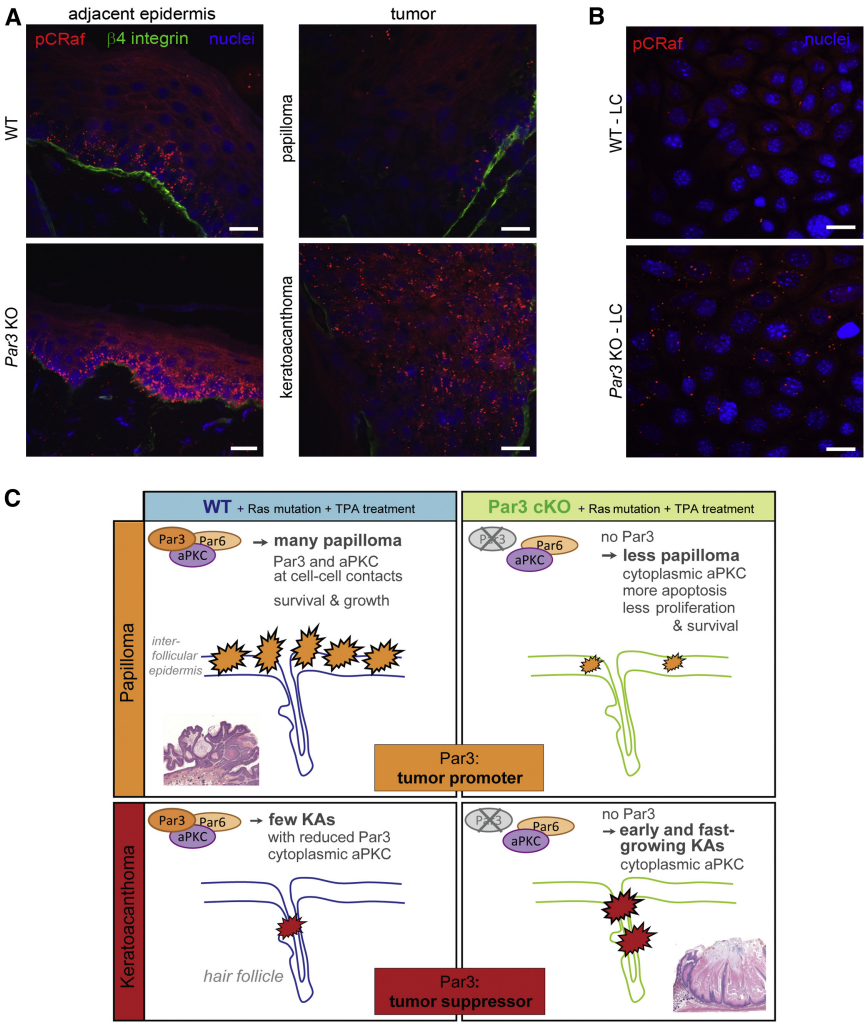


**Figure 7. Altered Localization and Activity of CRaf in Par3-Deficient Epidermis and Skin Tumors**

(A) Immunofluorescent staining of phosphorylated CRaf, reflecting the active form of CRaf in WT and *Par3* KO epidermis and tumor tissues. Scale bars, 20 μm.

(B) Immunofluorescent staining of phosphorylated CRaf in WT and *Par3* KO keratinocytes cultured at LC conditions. Scale bars, 20 μm.

(C) Model representing experimental skin tumorigenesis in WT and *Par3* KO mice. While papillomas likely arise mostly from suprabasal layers of the interfollicular epidermis, KAs are considered to originate from the hair follicle (Perez-Losada and Balmain, 2003). In WT epidermis and papillomas, Par3 and aPKC localize to intercellular adhesions. In the absence of Par3, papilloma formation and growth is reduced, which correlates with mislocalization of aPKC and components of the Ras pathway, impaired proliferation and survival signaling, and increased apoptosis, indicating tumor-promoting functions of Par3. In contrast, *Par3* KO mice develop significantly more KAs, suggesting a tumor-suppressive function of Par3 in hair follicular cells giving rise to KAs. This highlights opposing functions of Par3 in tumorigenesis depending on the tumor origin.

established human SCCs, in contrast to KAs (Figures 6G, 6H, and S4E), suggesting that the impact of Par3 expression on SCC formation is different as compared to KA formation. This leaves the possibility that Par3 function can be replaced by as yet unknown proteins in SCC but not KA formation.

The origin and development of KAs are not well understood. Proliferating cells of the basal and suprabasal layers of the interfollicular epidermis and the subsets of cells in the hair follicle each face a different microenvironment, which may eventually define the tumor outcome in pathologic conditions. Predominant expression of oncogenic Ras in differentiated interfollicular keratinocytes and subsequent tumor promotion induces papillomas (Bailleul et al., 1990; Greenhalgh et al., 1993; Owens and Watt, 2003). In contrast, expression of Ras in basal cells of the hair follicle results in the formation of KAs and SCCs that are independent of exogenous tumor promotion (Brown et al., 1998), indicating that the cell of KA origin resides in the hair follicle and shows little differentiation (Perez-Losada and Balmain, 2003). Par3 is expressed throughout the interfollicular epidermis and hair follicle but may act at different intracellular sites in cells giving rise to papillomas and KAs, respectively. Such cell type specific functions could explain the opposing tumor outcome observed in *Par3* KO mice (Figure 6D). While the formation of papillomas correlates with robust Par3 expression and localization to cell-cell contacts (Figures 1G and 6E), Par3 is strongly reduced in KAs and is rarely found at intercellular contact sites (Figure 6E). The differential outcome of Par3 deficiency on papilloma versus KA formation in vivo intriguingly parallels our observation that Par3 promotes growth and survival signaling in vitro only when cell-cell contacts are established. At LC conditions when Par3 is not enriched at cellular junctions it does not stimulate ERK, as *Par3* KO cells at these conditions show ERK activity equal to WT cells (Figure S3A). This suggests that junctional, but not cytoplasmic Par3, promotes cell survival and growth signaling, possibly by recruiting other proteins to intercellular adhesions. Indeed, we found that several components of the Ras-MAPK signaling pathway, including Ras, its GEF Sos2, and its effector pERK, localize to cell-cell contacts

(G) PAR3 expression in human epidermis and KA (paraffin sections). Colored boxes in overview indicate insets of KA (black) and epidermal (red) tissue. Scale bar, 100 μm.

(H) Quantification of PAR3 expression in human KAs and SCCs compared to adjacent epidermis (cryo sections). Related examples of micrographs see Figure S4B. Mean ± SEM; $^{**}p < 0.02$; $^{***}p < 0.001$.

See also Figure S4 and Table S1.

in a Par3-dependent manner, and loss of Par3 results in reduced ERK activation in cells with established cell-cell contacts. Interestingly, in human intestinal epithelial cells cortical active ERK1/2 has been recently associated with a stronger EGF-induced ERK activation as compared to cytoplasmic ERK in under-differentiated cells (Basuroy et al., 2006; Aggarwal et al., 2011). Moreover, we found that Par3 associates with aPKC in keratinocytes and observed Par3-dependent localization of aPKC to intercellular contacts both in vitro and in vivo. Importantly, in *Drosophila*, cortical aPKC induces neuroblast overgrowth, whereas cytoplasmic aPKCι is associated with poor prognosis in human ovarian and breast cancer (Grifoni et al., 2007; Kojima et al., 2008). aPKCι also mediates tumor cell growth, transformation and invasion in vitro and in experimental Ras-induced lung tumorigenesis likely by stimulating ERK signaling (Regala et al., 2009). Interestingly, ERK activity in *Par3* KO keratinocytes can be efficiently blocked by aurothiomalate (ATM) (Figure S3C), a small molecule inhibitor of the aPKC/Par6 interaction previously demonstrated to block oncogenic functions of aPKC in lung cancer (Erdogan et al., 2006; Stallings-Mann et al., 2006), indicating that in the absence of Par3 cytoplasmic aPKC can mediate ERK activity via interaction with Par6. Together, these data suggest that junctional aPKC contributes to Par3- and Ras-mediated growth and survival during papilloma formation, whereas increased KA formation as a result of loss of Par3 may involve oncogenic activities of cytoplasmic aPKC, likely in complex with Par6.

The Ras-based skin tumor model combined with loss of Par3 presented in this study provides a robust tool to study keratoacanthoma formation. Preclinical and clinical studies testing inhibitors of mutant BRaf to restrict metastatic growth of solid tumors recently provided evidence that human KAs also result from deregulated Ras signaling: 15%–31% of patients treated with the BRaf inhibitor vemurafenib (PLX4032, Roche, and Plexxikon) develop KAs or SCCs as adverse effect (Flaherty et al., 2010; Chapman et al., 2011). The *HRas* codon 61 mutation has recently, among other *Ras* mutations, been confirmed in those drug-promoted KAs harboring WT *BRaf* alleles (Oberholzer et al., 2012; Su et al., 2012). Moreover, in the DMBA/TPA mouse tumor model, which similarly induces *HRas* codon 61 mutations, vemurafenib treatment accelerated the growth of Ras-containing lesions accompanied by increased MAPK activity (Su et al., 2012), confirming that verumafenib indeed activates growth signaling in *Ras* mutant cells in vivo. BRaf inhibitors likely induce the formation of Raf dimers that leads to paradoxic CRaf activation and consequently MAPK pathway hyperactivation (Poulikakos et al., 2010; Hatzivassiliou et al., 2010; Heidorn et al., 2010). The observation of reduced Par3 expression in both mouse and human KAs (Figures 6E, 6F, 6H, and S4B) and of CRaf hyperactivation in Par3-deficient KAs (Figure 7A) therefore suggests a common mechanism of KA formation in human and mice involving *Ras* mutation and Par3 dysfunction.

In conclusion, we identified a tumor type-dependent function of Par3 in Ras-mediated skin cancer, with (pro)oncogenic and tumor-suppressive activity during papilloma and KA formation, respectively (Figure 7C). Our data underscore an important context-dependent role of polarity proteins in mammalian tumorigenesis and underlying signaling pathways. Our data further suggest that polarity protein dysfunction may differentially affect the tumor outcome in other tissues depending on the cellular context. In addition, we present a mouse tumor model of KA formation that recapitulates a human skin cancer of increasing clinical relevance.

## EXPERIMENTAL PROCEDURES

### Epidermal Par3 Deletion

To delete *Par3* specifically in the epidermis and hair follicle, mice with a conditional *Par3* allele (Hirose et al., 2006) were crossed with *K14-Cre(neo)* (Huelsken et al., 2001) mice. For further details see Supplemental Information. All experiments involving animals in this study were reviewed and approved by the Animal Experiments and Ethics Committee (DEC) of the Netherlands Cancer Institute and conformed the regulatory standards of the Dutch Act on Use of Laboratory animals.

### Skin Tumorigenesis Experiments

Two independent DMBA/TPA-mediated two-stage chemical skin carcinogenesis experiments were performed as previously described (Malliri et al., 2002). 25 WT (*K14-Cre*$^{+}$;*Par3*$^{wt/wt}$) and 27 *Par3* cKO (*K14-Cre*$^{+}$;*Par3*$^{flox/flox}$) mice of mixed genetic background have been used initially, and a repeat experiment comprised 17 WT and 11 *Par3* cKO mice of FVB background (F8). Results were essentially the same, and representative data are shown. Mice were examined twice a week, and tumor numbers and sizes were measured. At termination, normal skin, tumor tissue, and other organs were snap-frozen or fixed for further analyses.

### Tissue Processing, Histology, and Immunohistochemistry

Hematoxylin and eosin (H&E) staining and immunohistochemistry of normal skin and skin tumors were performed on formalin- or EAF-fixed 4 μm paraffin sections or 8 μm cryosections. For biochemical analysis, normal skin and tumor tissue was minced, collected in a tube and supplemented with radioimmunoprecipitation assay buffer containing protease inhibitor cocktail (SIGMA) and phosphatase inhibitors (Roche). The tissue was dissociated using a tissue homogenizator, incubated for 10 min on ice and then cleared by centrifugation. Alternatively, proteins were isolated in parallel to DNA and RNA using TRIzol Reagent according to the manufacturer's protocol (Invitrogen). Epidermal lysates were prepared from newborn and adult epidermis. Newborn epidermis was separated from the dermis after floating back-skin on ice-cold 0.5 M ammonium thiocyanate/PBS for 20 min, and adult epidermis was mechanically scraped-off the dermis. The epidermis was subsequently minced and proteins were isolated using TRIzol Reagent.

The use of human specimen involved in this study was approved by the institutional review board at the Medical Faculty of the University of Cologne. Written informed consent was obtained from patients in accordance with institutional review board policies and procedures for research dealing with tumor specimen.

### Apoptosis in Mouse Epidermis

DMBA (25 ug) or TPA ($10^{-4}$M) or both were applied to the backs of six mice of each genotype, and mice were killed 24 hr later. Apoptotic cells in skin biopsy specimen were detected by immunohistochemistry against cleaved caspase-3. The number of positively stained cells within the epidermis was evaluated per millimeter of basement membrane using phase-contrast microscopy of at least 60 nonserial tissue sections and subsequent image analysis (Aperio, Slidepath).

### Cell Proliferation in Mouse Epidermis

Control and *Par3* cKO littermates (n = 6 each) were treated with TPA alone ($10^{-4}$ M), DMBA alone (25 μg) for 24 hr, or were treated with DMBA and subsequently treated with two doses of TPA over 7 days. At the end of the experiment, mice were injected intraperitoneally with BrdU (Sigma) at 50 mg/kg, and killed 3 hr later. Using an anti-BrdU antibody (DAKO), the number of BrdU-stained cells within the epidermis was evaluated per millimeter of basement membrane using phase-contrast microscopy of at least 30 nonserial tissue sections and subsequent image analysis (Aperio and Slidepath).

Similarly, the thickness of the interfollicular epidermis was measured as readout for net proliferation.

### Antibodies

The following antibodies were used in this study: rabbit polyclonal antibodies directed against Par3 aa712-936 (Iden et al., 2006) and commercial sources (Millipore/Upstate, no. 07-330, and SIGMA-Aldrich HPA030443), aPKCzeta (C-20, Santa Cruz), PARP (no. 9542), phospho-p42/44 (Cell Signaling, no. 4370), pAkt Ser473 (Cell Signaling, no. 4060), ZO-1 (no. 61-7300, Invitrogen), cleaved caspase-3 (Cell Signaling, no. 9661), mouse-specific caspase 9 (Cell Signaling no. 9504), cyclin D1 (Upstate no. 05-815), Tiam1 (C-16, Santa Cruz), Keratin-1 (Covance, PRB149P), Tom20 (Santa Cruz, no. sc-11415), murine Bax (BD PharMingen, no. 554106), HA-tag (Y-11, Santa Cruz, no. sc-805), pcRAF Ser338 (Cell Signaling, no. 9427), Sos2 (Santa Cruz, no. sc-258), mouse monoclonal antibodies against ZO-1 (Invitrogen, no. 33-9100), Ras (BD Transduction, no. R02120), Ras (Ab-3, Millipore, no. OP-40), Rac1 (Upstate, clone 23A8, no. 05-389), ERK2 (BD Transduction, no. 610103), α-tubulin (SIGMA-Aldrich, no. T-5168, clone B-5-1-2), BrdU (DakoCytomation, no. MO744), E-cadherin (no. 610181, BD Transduction), β-catenin (BD Transduction, no. 610154), active Bax (clone 6A7, BD Pharmingen no. 556467), aPKCzeta (H-1, Santa Cruz, no. sc-17781), aPKCl/i (BD Transduction Labs, no. P20520, clone 23), HA-tag (12CA5, own hybridoma), HA-probe (F-7, Santa Cruz, no. sc-7392). For secondary detection, species-directed antibodies conjugated with AlexaFluor fluorophors (Molecular Probes) or horse radish peroxidase (GE Healthcare) were used for immunofluorescence or western blot studies, respectively.

### Isolation of Primary Mouse Keratinocytes

Primary murine keratinocytes were isolated from newborn *Par3*$^{flox/flox}$ mice and cultured as previously described (Mertens et al., 2005), whereby epidermal and dermal fractions were kept separate. Primary and SV40-immortalized epidermal and dermal cells expressing typical keratinocyte marker proteins have been used in this study. Cells were plated on Collagen I-coated dishes and used up to passage 20. *Par3* was deleted by retroviral infection with self-excising Cre recombinase (Silver and Livingston, 2001). Corresponding parental cell isolations of identical passage served as control.

### Tumor Promoter Treatments In Vitro

Keratinocytes were growth factor-starved for 2 hr, and then treated with either 40 ng/ml murine epidermal growth factor (BD Biosciences) or 0.68 μM TPA (SIGMA-Aldrich) for indicated time points. Lysates of adherent and floating cells were combined for subsequent biochemical analysis.

### Colony Formation Assays

Cold growth factor-reduced matrigel (BD Biosciences) was diluted 1:1 in keratinocyte culture medium and 30 μl were pipetted into a chilled 96 well plate. Subconfluent keratinocytes were harvested by trypsinization, counted and seeded into a matrigel matrix to yield a final concentration of $5 \times 10^3$ cells/ml. The matrigel:cell mix was incubated at 37°C for 45 min to solidify the matrigel. Afterward, culture medium was added to the top and replaced every second day. Colony formation was followed over a period of up to 3 weeks.

### Immunofluorescence Analysis: Mono- and Multilayer Tissue

For monolayer cultures, keratinocytes were seeded on Collagen I-coated 8 well or 16 well LabTek Chamber Slides (Nunc), grown until confluency and then switched to NC levels (2mM). For analysis of multilayer cultures, keratinocytes were seeded on Collagen I-coated TransWell Filters (TransWell Clear, 0.4 μm pore size, 6.5 mm diameter, Nunc), grown to confluency and then incubated at NC levels for several days. For immunofluorescence staining, monolayer and multilayer cultures were washed twice with PBS and fixed with either PFA (4% PFA in PBS 10 min at room temperature, followed by 15 min 0.5% Triton X-100 in PBS for permeabilization) or ethanol/acetone (30 min 96% ethanol on ice, followed by 3 min incubation of ice-cold acetone at RT). Cells were blocked with 5% BSA for 1 hr at RT, and subsequently incubated with primary antibodies diluted in AB buffer (10 mM Tris-HCl, 150 mM NaCl, and 0.1% BSA) in a humidified chamber overnight at 4°C. Incubation with AlexaFluor 488- and 568-conjugated secondary antibodies (Invitrogen) and TOPRO as nuclei stain (Invitrogen) was carried out for 1 hr at room temperature in AB buffer. Immunostained cells on chamber slides were mounted in Mowiol; filters with multilayer cultures were first excised and then mounted to a glass slide.

Additional experimental procedures can be found in Supplemental Experimental Procedures.

## SUPPLEMENTAL INFORMATION

Supplemental Information includes four figures, one table, and Supplemental Experimental Procedures and can be found with this article online at http://dx.doi.org/10.1016/j.ccr.2012.08.004.

## ACKNOWLEDGMENTS

We thank Carien Niessen and Klaus Ebnet for critically reading the manuscript. We are grateful to the NKI facilities for experimental animals, animal pathology, and digital microscopy and to the CECAD Imaging Facility in Cologne for professional support. We acknowledge Jelle Wesseling and Mark Opdam (NKI), Cornelia Mauch and Paola Zigrino (Z2 project SFB829) for providing human skin tumor samples, and Klaus Ebnet, Carien Niessen, Susanne Vorhagen, Ian Macara, David M. Livingston, and Hamid Kashkar for constructs and reagents. Furthermore, we thank members of the Division of Cell Biology I for helpful discussions and Rehan Villani for linguistic advice. This work was supported by the European Commission (TuMIC), the Dutch Cancer Society (KWF), the excellence initiative by the German federal and state governments (CECAD Cologne), and the German Research Foundation (CRC829 and CRC832).

Received: September 26, 2011
Revised: January 31, 2012
Accepted: August 6, 2012
Published: September 10, 2012

## REFERENCES

Aggarwal, S., Suzuki, T., Taylor, W.L., Bhargava, A., and Rao, R.K. (2011). Contrasting effects of ERK on tight junction integrity in differentiated and under-differentiated Caco-2 cell monolayers. Biochem. J. *433*, 51–63.

Assémat, E., Bazellières, E., Pallesi-Pocachard, E., Le Bivic, A., and Massey-Harroche, D. (2008). Polarity complex proteins. Biochim. Biophys. Acta *1778*, 614–630.

Bailleul, B., Surani, M.A., White, S., Barton, S.C., Brown, K., Blessing, M., Jorcano, J., and Balmain, A. (1990). Skin hyperkeratosis and papilloma formation in transgenic mice expressing a ras oncogene from a suprabasal keratin promoter. Cell *62*, 697–708.

Basuroy, S., Seth, A., Elias, B., Naren, A.P., and Rao, R. (2006). MAPK interacts with occludin and mediates EGF-induced prevention of tight junction disruption by hydrogen peroxide. Biochem. J. *393*, 69–77.

Bilder, D. (2004). Epithelial polarity and proliferation control: links from the Drosophila neoplastic tumor suppressors. Genes Dev. *18*, 1909–1925.

Brown, K., Strathdee, D., Bryson, S., Lambie, W., and Balmain, A. (1998). The malignant capacity of skin tumours induced by expression of a mutant H-ras transgene depends on the cell type targeted. Curr. Biol. *8*, 516–524.

Cain, R.J., and Ridley, A.J. (2009). Phosphoinositide 3-kinases in cell migration. Biol Cell. *1*, 13–29.

Chapman, P.B., Hauschild, A., Robert, C., Haanen, J.B., Ascierto, P., Larkin, J., Dummer, R., Garbe, C., Testori, A., Maio, M., et al; BRIM-3 Study Group. (2011). Improved survival with vemurafenib in melanoma with BRAF V600E mutation. N. Engl. J. Med. *364*, 2507–2516.

Chen, X., and Macara, I.G. (2005). Par-3 controls tight junction assembly through the Rac exchange factor Tiam1. Nat. Cell Biol. *7*, 262–269.

Cho, S.H., Delehedde, M., Rodriguez-Villanueva, J., Brisbay, S., and McDonnell, T.J. (2001). Bax gene disruption alters the epidermal response to ultraviolet irradiation and in vivo induced skin carcinogenesis. Int. J. Mol. Med. *7*, 235–241.

Erdogan, E., Lamark, T., Stallings-Mann, M., Jamieson, L., Pellecchia, M., Thompson, E.A., Johansen, T., and Fields, A.P. (2006). Aurothiomalate inhibits

transformed growth by targeting the PB1 domain of protein kinase Ciota. J. Biol. Chem. *281*, 38450–9.

Filmus, J., Robles, A.I., Shi, W., Wong, M.J., Colombo, L.L., and Conti, C.J. (1994). Induction of cyclin D1 overexpression by activated ras. Oncogene *9*, 3627–3633.

Finch, J.S., Albino, H.E., and Bowden, G.T. (1996). Quantitation of early clonal expansion of two mutant 61st codon c-Ha-ras alleles in DMBA/TPA treated mouse skin by nested PCR/RFLP. Carcinogenesis *17*, 2551–2557.

Flaherty, K.T., Puzanov, I., Kim, K.B., Ribas, A., McArthur, G.A., Sosman, J.A., O'Dwyer, P.J., Lee, R.J., Grippo, J.F., Nolop, K., and Chapman, P.B. (2010). Inhibition of mutated, activated BRAF in metastatic melanoma. N. Engl. J. Med. *363*, 809–819.

Greenhalgh, D.A., Rothnagel, J.A., Quintanilla, M.I., Orengo, C.C., Gagne, T.A., Bundman, D.S., Longley, M.A., and Roop, D.R. (1993). Induction of epidermal hyperplasia, hyperkeratosis, and papillomas in transgenic mice by a targeted v-Ha-ras oncogene. Mol. Carcinog. *7*, 99–110.

Grifoni, D., Garoia, F., Bellosta, P., Parisi, F., De Biase, D., Collina, G., Strand, D., Cavicchi, S., and Pession, A. (2007). aPKCzeta cortical loading is associated with Lgl cytoplasmic release and tumor growth in Drosophila and human epithelia. Oncogene *26*, 5960–5965.

Hatzivassiliou, G., Song, K., Yen, I., Brandhuber, B.J., Anderson, D.J., Alvarado, R., Ludlam, M.J., Stokoe, D., Gloor, S.L., Vigers, G., et al. (2010). RAF inhibitors prime wild-type RAF to activate the MAPK pathway and enhance growth. Nature *464*, 431–435.

Heidorn, S.J., Milagre, C., Whittaker, S., Nourry, A., Niculescu-Duvas, I., Dhomen, N., Hussain, J., Reis-Filho, J.S., Springer, C.J., Pritchard, C., and Marais, R. (2010). Kinase-dead BRAF and oncogenic RAS cooperate to drive tumor progression through CRAF. Cell *140*, 209–221.

Hirose, T., Karasawa, M., Sugitani, Y., Fujisawa, M., Akimoto, K., Ohno, S., and Noda, T. (2006). PAR3 is essential for cyst-mediated epicardial development by establishing apical cortical domains. Development *133*, 1389–1398.

Horikoshi, Y., Suzuki, A., Yamanaka, T., Sasaki, K., Mizuno, K., Sawada, H., Yonemura, S., and Ohno, S. (2009). Interaction between PAR-3 and the aPKC-PAR-6 complex is indispensable for apical domain development of epithelial cells. J. Cell Sci. *122*, 1595–1606.

Huang, L., and Muthuswamy, S.K. (2010). Polarity protein alterations in carcinoma: a focus on emerging roles for polarity regulators. Curr. Opin. Genet. Dev. *20*, 41–50.

Huelsken, J., Vogel, R., Erdmann, B., Cotsarelis, G., and Birchmeier, W. (2001). beta-Catenin controls hair follicle morphogenesis and stem cell differentiation in the skin. Cell *105*, 533–545.

Iden, S., and Collard, J.G. (2008). Crosstalk between small GTPases and polarity proteins in cell polarization. Nat. Rev. Mol. Cell Biol. *9*, 846–859.

Iden, S., Rehder, D., August, B., Suzuki, A., Noda, K., Nagafuchi, A., Wolburg-Buchholz, K., Wolburg, H., Ohno, S., et al. (2006). A distinct PAR polarity protein complex physically associated with VE-cadherin in vertebrate endothelial cells. EMBO Rep. *7*, 1239–1246.

Itoh, N., Nakayama, M., Nishimura, T., Fujisue, S., Nishioka, T., Watanabe, T., and Kaibuchi, K. (2010). Identification of focal adhesion kinase (FAK) and phosphatidylinositol 3-kinase (PI3-kinase) as Par3 partners by proteomic analysis. Cytoskeleton (Hoboken). *5*, 297–308.

Kern, F., Niault, T., and Baccarini, M. (2011). Ras and Raf pathways in epidermis development and carcinogenesis. Br. J. Cancer *104*, 229–234.

Kojima, Y., Akimoto, K., Nagashima, Y., Ishiguro, H., Shirai, S., Chishima, T., Ichikawa, Y., Ishikawa, T., Sasaki, T., Kubota, Y., et al. (2008). The overexpression and altered localization of the atypical protein kinase C lambda/iota in breast cancer correlates with the pathologic type of these tumors. Hum. Pathol. *39*, 824–831.

Macara, I.G. (2004). Par proteins: partners in polarization. Curr. Biol. *14*, R160–R162.

Malliri, A., van der Kammen, R.A., Clark, K., van der Valk, M., Michiels, F., and Collard, J.G. (2002). Mice deficient in the Rac activator Tiam1 are resistant to Ras-induced skin tumours. Nature *417*, 867–871.

Mertens, A.E., Rygiel, T.P., Olivo, C., van der Kammen, R., and Collard, J.G. (2005). The Rac activator Tiam1 controls tight junction biogenesis in keratinocytes through binding to and activation of the Par polarity complex. J. Cell Biol. *170*, 1029–1037.

Morais-de-Sá, E., Mirouse, V., and St Johnston, D. (2010). aPKC phosphorylation of Bazooka defines the apical/lateral border in Drosophila epithelial cells. Cell *141*, 509–523.

Murray, N.R., Kalari, K.R., and Fields, A.P. (2011). Protein kinase Cι expression and oncogenic signaling mechanisms in cancer. J. Cell. Physiol. *226*, 879–887.

Nolan, M.E., Aranda, V., Lee, S., Lakshmi, B., Basu, S., Allred, D.C., and Muthuswamy, S.K. (2008). The polarity protein Par6 induces cell proliferation and is overexpressed in breast cancer. Cancer Res. *68*, 8201–8209.

Oberholzer, P.A., Kee, D., Dziunycz, P., Sucker, A., Kamsukom, N., Jones, R., Roden, C., Chalk, C.J., Ardlie, K., Palescandolo, E., et al. (2012). RAS mutations are associated with the development of cutaneous squamous cell tumors in patients treated with RAF inhibitors. J. Clin. Oncol. *30*, 316–321.

Owens, D.M., and Watt, F.M. (2003). Contribution of stem cells and differentiated cells to epidermal tumours. Nat. Rev. Cancer *3*, 444–451.

Pagliarini, R.A., and Xu, T. (2003). A genetic screen in Drosophila for metastatic behavior. Science *302*, 1227–1231.

Partanen, J.I., Tervonen, T.A., Myllynen, M., Lind, E., Imai, M., Katajisto, P., Dijkgraaf, G.J., Kovanen, P.E., Mäkelä, T.P., Werb, Z., and Klefström, J. (2012). Tumor suppressor function of Liver kinase B1 (Lkb1) is linked to regulation of epithelial integrity. Proc. Natl. Acad. Sci. USA *109*, E388–E397.

Pearson, H.B., Perez-Mancera, P.A., Dow, L.E., Ryan, A., Tennstedt, P., Bogani, D., Elsum, I., Greenfield, A., Tuveson, D.A., Simon, R., and Humbert, P.O. (2011). SCRIB expression is deregulated in human prostate cancer, and its deficiency in mice promotes prostate neoplasia. J. Clin. Invest. *121*, 4257–4267.

Pegtel, D.M., Ellenbroek, S.I., Mertens, A.E., van der Kammen, R.A., de Rooij, J., and Collard, J.G. (2007). The Par-Tiam1 complex controls persistent migration by stabilizing microtubule-dependent front-rear polarity. Curr. Biol. *17*, 1623–1634.

Perez-Losada, J., and Balmain, A. (2003). Stem-cell hierarchy in skin cancer. Nat. Rev. Cancer *3*, 434–443.

Poulikakos, P.I., Zhang, C., Bollag, G., Shokat, K.M., and Rosen, N. (2010). RAF inhibitors transactivate RAF dimers and ERK signalling in cells with wild-type BRAF. Nature *464*, 427–430.

Regala, R.P., Davis, R.K., Kunz, A., Khoor, A., Leitges, M., and Fields, A.P. (2009). Atypical protein kinase Ciota is required for bronchioalveolar stem cell expansion and lung tumorigenesis. Cancer Res. *69*, 7603–7611.

Reischauer, S., Levesque, M.P., Nüsslein-Volhard, C., and Sonawane, M. (2009). Lgl2 executes its function as a tumor suppressor by regulating ErbB signaling in the zebrafish epidermis. PLoS Genet. *5*, e1000720.

Reuter, J.A., Ortiz-Urda, S., Kretz, M., Garcia, J., Scholl, F.A., Pasmooij, A.M., Cassarino, D., Chang, H.Y., and Khavari, P.A. (2009). Modeling inducible human tissue neoplasia identifies an extracellular matrix interaction network involved in cancer progression. Cancer Cell *15*, 477–488.

Rizzo, M.A., Kraft, C.A., Watkins, S.C., Levitan, E.S., and Romero, G. (2001). Agonist-dependent traffic of raft-associated Ras and Raf-1 is required for activation of the mitogen-activated protein kinase cascade. J. Biol. Chem. *276*, 34928–34933.

Silver, D.P., and Livingston, D.M. (2001). Self-excising retroviral vectors encoding the Cre recombinase overcome Cre-mediated cellular toxicity. Mol. Cell *8*, 233–243.

Stallings-Mann, M., Jamieson, L., Regala, R.P., Weems, C., Murray, N.R., and Fields, A.P. (2006). A novel small-molecule inhibitor of protein kinase Ciota blocks transformed growth of non-small-cell lung cancer cells. Cancer Res. *66*, 1767–1774.

Su, F., Viros, A., Milagre, C., Trunzer, K., Bollag, G., Spleiss, O., Reis-Filho, J.S., Kong, X., Koya, R.C., Flaherty, K.T., et al. (2012). RAS mutations in cutaneous squamous-cell carcinomas in patients treated with BRAF inhibitors. N. Engl. J. Med. *366*, 207–215.

Vaahtomeri, K., and Mäkelä, T.P. (2011). Molecular mechanisms of tumor suppression by LKB1. FEBS Lett. *585*, 944–951.

Van Laethem, A., Van Kelst, S., Lippens, S., Declercq, W., Vandenabeele, P., Janssens, S., Vandenheede, J.R., Garmyn, M., and Agostinis, P. (2004). Activation of p38 MAPK is required for Bax translocation to mitochondria, cytochrome c release and apoptosis induced by UVB irradiation in human keratinocytes. FASEB J. *18*, 1946–1948.

Wang, Z., Pedersen, E., Basse, A., Lefever, T., Peyrollier, K., Kapoor, S., Mei, Q., Karlsson, R., Chrostek-Grashoff, A., and Brakebusch, C. (2010). Rac1 is crucial for Ras-dependent skin tumor formation by controlling Pak1-Mek-Erk hyperactivation and hyperproliferation in vivo. Oncogene *29*, 3362–3373.

Yoshimura, T., Arimura, N., and Kaibuchi, K. (2006). Signaling networks in neuronal polarization. J. Neurosci. *26*, 10626–10630.

Zhan, L., Rosenberg, A., Bergami, K.C., Yu, M., Xuan, Z., Jaffe, A.B., Allred, C., and Muthuswamy, S.K. (2008). Deregulation of scribble promotes mammary tumorigenesis and reveals a role for cell polarity in carcinoma. Cell *135*, 865–878.